Journal of Theoretical and Applied Physics (2019) 13:277–288
https://doi.org/10.1007/s40094-019-0336-1

RESEARCH

Heat capacity and entropy of Gaussian spherical quantum dot in the presence of donor impurity

Nehal S. Yahyah[1] · Mohammad K. Elsaid[1] · Ayham Shaer[1]

Received: 7 March 2019 / Accepted: 27 May 2019 / Published online: 4 June 2019

Abstract
The energy states of shallow donor impurity in GaAs/AlGaAs quantum dot heterostructure with Gaussian potential have been calculated by the shifted 1/*N* expansion method. The effects of the impurity on the ground state energy and average statistical energy have been investigated. The present calculations show that the donor impurity modifies significantly the electron energy levels of spherical quantum dot and thermal properties. In addition, we have also displayed the variations of the heat capacity and entropy of donor impurity in quantum dot with the radius, confining potential depth, dimension and temperature. The comparison shows that our results are in very good agreement with the theoretical reported work.

Keywords Gaussian quantum dot · Impurity · Binding energy · Heat capacity · Entropy · 1/*N* expansion

Introduction

Nanoscience is a very interesting and technologically relevant area of condensed matter physics. With the development of modern technology, it is now possible to produce semiconductor nanostructures with different reduced dimensions like: zero-dimensional (0D), one-dimensional (1D) and two-dimensional (2D) systems. The zero-dimensional systems are called quantum dots (QDs). Quantum dot (QD) is a conducting land of ultra-small system in the area of electronics and optoelectronics. The carriers in QD are confined in all three dimensions; therefore, energy is discrete as in the natural atoms. New potential application in optoelectronics will be discovered by changing the electronic and optical properties of QDs which may be controlled by an appropriate selection of the sample geometry and material parameters, so the size and shape of quantum dots can be experimentally tuned over a wide range [1–7]. The physics of shallow donor impurity states in QDs is an interesting subject, so many theoretical and experimental studies of impurity-related properties in low-dimensional heterostructure have been reported in the last decade. This is because their presence can dramatically alter the performance of QDs and their optical and transport (electrical) properties. The binding energy of the hydrogenic impurity in the quantum dot is extensively studied [8–13]. Most of the theoretical works carried out on shallow donors in spherical quantum dots employ variational approaches [14], or alternatively, perturbation method limited to the strong confinement regime [15], while the exact solution has been obtained for centered impurities [16]. Zhu et al. [17, 18] solved the finite potential well for impurity in the center of spherical quantum dot and obtained the exact solution by using the method of series expansion. Bose et al. [19] obtained the binding energy of a shallow hydrogenic impurity in a spherical quantum dot with a parabolic potential shape by perturbation method. Using variational and fractional-dimensional space approaches, Porras-Montenegro et al. [20] have calculated the binding energy for shallow donor impurities in rectangular quantum dots for both finite and infinite potential confinement. A computational scheme yields to exact energies of a spherical nanocrystallite with a shallow donor impurity located anywhere inside are presented by Movilla and Planelles [21]. Different authors have solved the Schrodinger equation of the quantum dot with Gaussian confinement potential model [22–27]. For example, Gharaati and Khordad [28] used a modified Gaussian potential to calculate energy levels for spherical quantum dot within effective mass approximation. Boda et al. [29] investigated the Gaussian confinement of hydrogenic donor impurity by a very simple variational wave function. The method of 1/*N* expansion has been developed,

✉ Mohammad K. Elsaid
mkelsaid@najah.edu

[1] Physics Department, An-Najah National University, Nablus, West Bank, Palestine

which was proposed by Sukhatme and Imbo [30, 31] to calculate the spectra of an electron and a donor in QD. Elsaid [32, 33] had studied the quantum dot Hamiltonian by this method in different works. Al-Hayek used $1/N$ expansion to calculate energy and binding energy of donor impurity in quantum dot with Gaussian Confinement. The $1/N$ method is a powerful tool to solve Schrodinger equation for spherical symmetric potentials, and it is used in different branches of theoretical physics. The method gives accurate results of energy eigenvalues calculations of the system without dealing with trail wave functions. The $1/N$ expansion method is applicable to the entire range of the magnetic field strength, while the perturbation theory is limited to a weak range only.

In this work, we investigate the thermodynamic properties of a semiconductor GaAs Gaussian quantum dot and show the effect of donor impurity, quantum dot radius (R), confining potential depth (V_0), dimension (N) and temperature (T) on the heat capacity and entropy of a single electron in spherical QD in the presence of donor impurity with Gaussian confinement potential. The shifted $1/N$ expansion method has been used to solve QD Hamiltonian to obtain the eigenenergies as a necessary input data to calculate the physical properties of the QD. The rest of paper is organized as follows: The Hamiltonian of donor impurity in QD with Gaussian potential and the shifted $1/N$ solution method are presented in "Theory and method of calculation" section. In "Results" section, the results of energy and thermal quantities like heat capacity (C_v) and entropy (S) have been displayed and discussed, while the final "Conclusions" section is devoted to the conclusion.

Theory and method of calculation

The standard Hamiltonian of an electron in the presence of a hydrogenic donor located at the center of quantum dot can be written as follows:

$$\hat{H} = -\frac{\hbar^2}{2m^*}\nabla^2 - \frac{ze^2}{\epsilon r} - V_0 e^{-r^2/2R^2} \tag{1}$$

where V_0 is potential well depth, R is quantum dot radius (the range of the confinement potential), r is electron position coordinate, $r = (x, y)$ for the 2D and $r = (x, y, z)$ for the 3D. Coulomb attractive interaction between the donor electron and the hydrogenic nucleus is represented by the second term in Hamiltonian. $z = 0$ when the donor impurity is absented, and $z = 1$ as donor impurity is presented. Gaussian confining potential can be treated as parabolic potential plus a perturbation because the deviation of Gaussian confining from the parabolic potential is small enough. The solution of donor impurity Hamiltonian, Eq. (1), with Gaussian potential cannot be obtained in analytic closed form. In this paper, we intend to solve the Hamiltonian by using the shifted $1/N$ expansion method. The technique is efficient and accurate. The radial part Schrodinger equation in N-dimensional space can be expressed as:

$$\left[-\frac{\hbar^2}{2m^*}\left(\frac{\mathrm{d}^2}{\mathrm{d}r^2} + \frac{N-1}{r}\frac{\mathrm{d}}{\mathrm{d}r} - \frac{l(l+N-2)}{r^2}\right) + V(r)\right]\varphi(r) = E\varphi(r) \tag{2}$$

where

$$V(r) = -\frac{ze^2}{\epsilon r} - V_0 e^{-r^2/2R^2} \tag{3}$$

and m^* is electron effective mass, ϵ is the dielectric constant of the GaAs material, $\hbar$ is the reduced Planck Constant, and N is number of spatial dimensions. The term $l(l+N-2)\hbar^2$ is the eigenvalue of the square of the N-dimensional orbital angular momentum and $l = |m|$ where m is the magnetic quantum number ($m = 0, \mp1, \pm2, \ldots\ldots\ldots$) which labels the QD energy states. The first derivative term in N-dimensional Schrodinger equation, Eq. (2) can be removed by appropriate substitution:

$$\varphi(r) = r^{-\frac{N-1}{2}}u(r) \tag{4}$$

and the total QD wave function,

$$\Psi(r, \phi) = \varphi(r)e^{im\phi} \tag{5}$$

Equation (3) will take the following form:

$$\left(-\frac{\hbar^2}{2m^*}\frac{\mathrm{d}^2}{\mathrm{d}r^2} + \frac{(\bar{k}+a-1)(\bar{k}+a-3)\hbar^2}{8m^*r^2} + V(r)\right)u(r) = Eu(r) \tag{6}$$

where $\bar{k} = N + 2l - a$, and a is suitable shift parameter that can be determined later. To calculate the energy eigenvalues, $E(n, l)$, we will expand Schrodinger equation in terms of parameter $(\bar{k})$ and shift parameter (a). The complete mathematical steps that lead to the QD energy eigenvalues expressions in terms of powers of $1/\bar{k}$ are given in previous works [11–14], and it will not be repeated. The energy eigenvalues, $E(n, l)$, in powers of $1/\bar{k}$ (up to the third order) are given by:$E(n, l) = E_0 + E_1 + E_2 + E_3$. All the energy terms are determined in terms of the quantum numbers, the roots, and the potential derivatives.

The shift parameter a can be determined by making the term, E_1, vanish, namely $(E_1 = 0)$. This condition, in fact, guarantees that $1/N$ method gives exact energy results for both, harmonic oscillator and hydrogen Hamiltonians [30, 31],

$$a = 2 - 2(2n_r + 1)\frac{m^*\omega}{\hbar} \tag{7}$$

where ω is the harmonic frequency parameter given by:

$$\omega = \frac{\hbar}{2m^*}\left[3 + \frac{r_0 V''(r_0)}{V'(r_0)}\right]^{1/2} \tag{8}$$

Table 1 Eigenenergy states in units R_D for 3D quantum dot (spherical QD) without impurity and $V_0 = 400R_D$, dot radius $R = 1/\sqrt{2}a_D$, calculated by various computational methods

Energy spectra	Diagonalization techniques [35]	Numerov integration algorithm [35, 36]	Hypervirial-Pade method [37]	Present work [1/*N*]
1*s*	− 341.895	− 341.892	− 341.8952	− 341.895
1*p*	− 304.463	− 304.463	− 304.4628	− 304.463
2*s*	− 269.644	− 269.640	− 269.6445	− 269.644
1*d*	− 268.110	− 268.111	− 268.1107	− 268.111
2*p*	− 234.446	− 235.450	− 235.4500	− 235.451
1*f*	− 232.849	− 232.895	− 232.8753	− 232.878
3*s*	− 203.983	− 203.979	− 203.9835	− 203.997
2*d*	− 202.427	− 202.431	− 202.4313	− 202.432
1*g*	− 198.700	− 198.798	− 198.7983	− 198.798
3*p*	− 173.156	− 173.244	− 173.2443	− 173.257
2*f*	− 167.797	− 170.639	− 170.6393	− 170.640
4*s*	− 145.372	− 145.373	− 145.3779	− 145.431
3*d*	− 145.741	− 143.809	− 143.8091	− 143.821

For fixed quantum numbers: n_r and l and confinement potential V_0, the root r_0 is determined from the following relation:

$$N + 2l - 2 + \left(2n_r + 1\right)\left[3 + \frac{r_0 V''(r_0)}{V'(r_0)}\right]^{1/2} = \left[\frac{4m^* r_0^3}{\hbar^2} V'(r_0)\right]^{\frac{1}{2}} \tag{9}$$

Having determined r_0, we can compute, a and every identified parameter, which complete all necessary steps to calculate the energy spectra of the QD Hamiltonian.

The heat capacity and entropy

To calculate the heat capacity of the system, we have evaluated the mean energy from the statistical energy expression:

$$\left\langle E\left(T, V_0, R, N\right)\right\rangle = \frac{\sum_{j=1}^{n_{\max}} E_j e^{-\frac{E_j}{K_B T}}}{\sum_{j=1}^{n_{\max}} e^{-\frac{E_j}{K_B T}}} \tag{10}$$

Then heat capacity can be calculated from Eq. (10) by taking the temperature derivative of the mean energy:

$$C_v\left(T, V_0, R, N\right) = \frac{\partial\left\langle E\left(T, V_0, R, N\right)\right\rangle}{\partial T} \tag{11}$$

The entropy (S) can be calculated by equation:

$$S\left(T, V_0, R, N\right) = \frac{\partial(K_B T \ln\left\langle Z\left(T, V_0, R, N\right)\right\rangle)}{\partial T} \tag{12}$$

where:

$$\left\langle Z\left(T, V_0, R, N\right)\right\rangle = \sum_{j=1}^{n_{\max}} e^{-E_j/K_B T} \tag{13}$$

Results

In this work, the effective atomic units are used so that all energies of QD system made from GaAs/AlGaAs heterostructure are measured in units of donor effective Rydberg (R_D) and all distances are measured in units of donor effective Bohr radius (a_D). The eigenenergies of the donor impurity in three-dimensional (3D) spherical quantum dot obtained by 1/*N* expansion method against different computation methods are listed in Table 1 for $V_0 = 400\,R_D$ and dot radius $R = 1/\sqrt{2}a_D$. The analytic expression for the energies $E(n, l)$ yields accurate results for a wide range values of states: (n, l) in comparison with all computational methods that had been implemented to solve the Schrodinger equation for QD system. The tabulated results clearly show the accuracy of 1/*N* expansion against various computational methods: diagonalizing, Numerov integration algorithm and Hypervirial-Pade methods.

In Fig. 1, we plot the computed ground state energy $E(1, 0)$ results of this work against the radius of 3D QD (R) for both with impurity and without impurity. The energy with impurity and without impurity has a similar dependence on (R). As the QD radius (R) decreases, the state energy of the QD increases monotonically. The electron wave function is mainly distributed inside the well region of the QD, so the existence of impurity leads to the increase in the energy. In this case, the Coulomb attractive energy enhances, since the separation distance between the electron and the impurity, which is located at the center of the QD, becomes small. For example, the QD ground state energy changes from $E \approx -35R_D$ to $E \approx -40R_D$ at QD radius $R = 1a_D$ [34]. The impurity modifies the energy levels of QDs and it affects their electronic and optical properties.

In Fig. 2, we show the behavior of average statistical energy of 3D QD with and without donor impurity as a

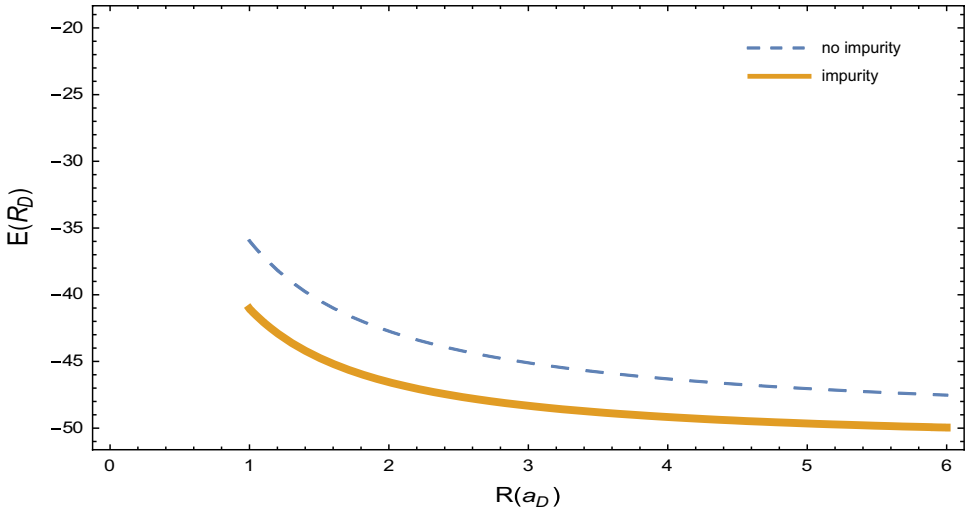

Fig. 1 Ground state energy $E(1,0)$ in QD as a function of dot radius (R) for $V_0 = 50R_D, N = 3D$ with impurity and without impurity

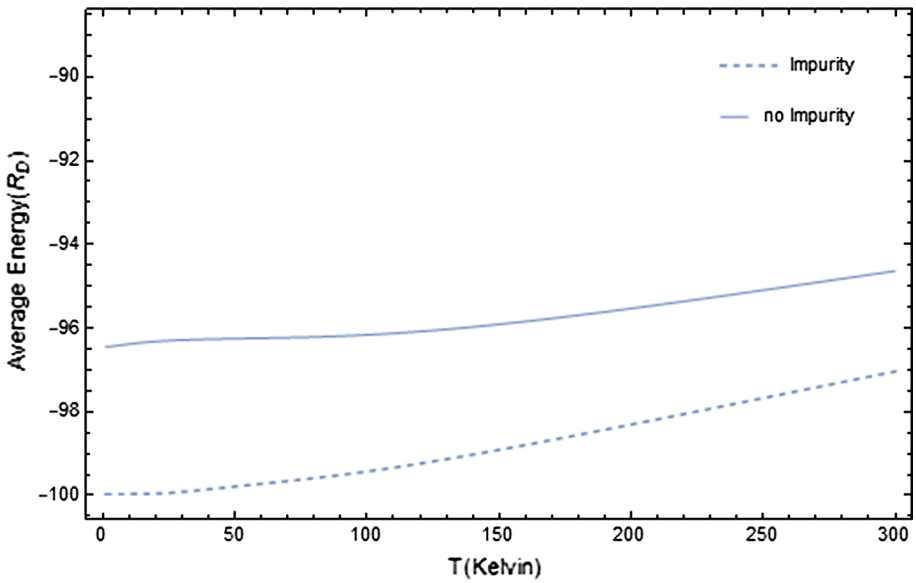

Fig. 2 Average energy of QD as a function of temperature (T) with donor impurity and without impurity at $R = 2a_D, V_0 = 100R_D, N = 3D$

function of temperature (T). We observe that the average thermodynamic energy increases with increasing temperature (T). The reason for this behavior is due to the significant increment in the thermal and the confinement energy contributions. The behavior of the average energy in QD depends on the density of states because the energy levels are discrete; consequently, the thermodynamic properties will depend on the energy-level distribution and temperature (T) of the occupation probability of the states. The donor impurity increases the average energy due to its negative Coulomb contribution between the electron and the nucleus of the donor impurity.

In Fig. 3, we plot also the average statistical energy as a function of temperature for different number of eigenenergy bases (n_{max}) to assure that the calculated average energy is a converging quantity. For example, we can see at low temperature range, only small number of basis is needed. However, for high temperature, we need a large number of bases to achieve a numerically stable converging energy for the QD system. These results are in agreement with the corresponding ones given very recently in Figure 12 of Nammas' work [38].

The donor impurity binding energy $E_B(n,l)$ in a given state is defined as usual, and the difference between energy of the QD Hamiltonian in the absence and presence of the donor impurity is: $E_B(n,l) = E_B(n,l,z=0) - E_B(n,l,z=1)$. Figure 4 shows the effect of the temperature (T) on the average binding energy of QD. Due to the enhancement of the electron spatial probability density at low temperature (T), it is found that at low temperature (T) of 4 K the average binding energy is increased over that associated with temperature (T) near room 300 K. At low temperatures, the thermal energy of the system is less than the Coulomb interaction which means the increase in the binding energy, but as the temperature increases than 20 K, the kinetic energy (more thermal energy) will be more than the Coulomb interaction and that leads to

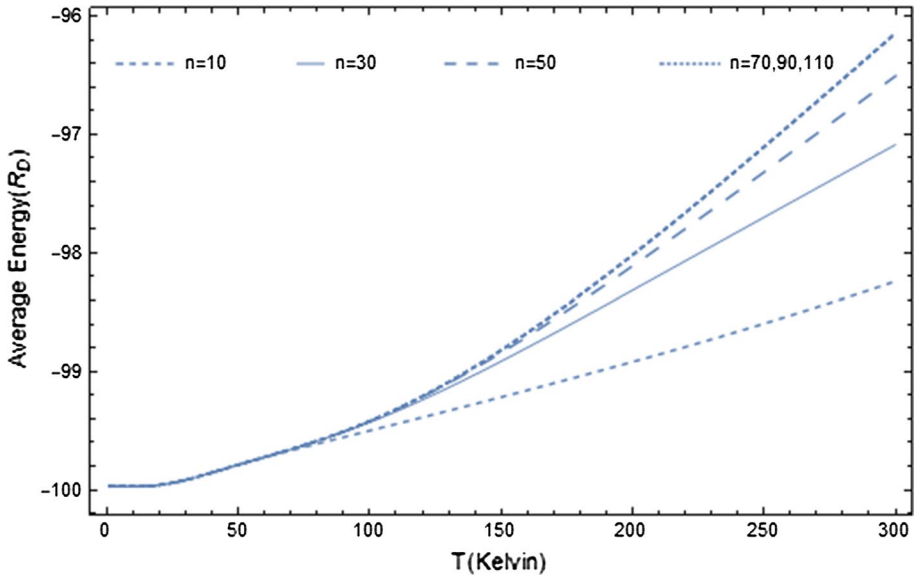

Fig. 3 Average energy of QD as a function of temperature (T) with donor impurity for different n_{max} at $R = 2a_D, V_0 = 100R_D, N = 3D$

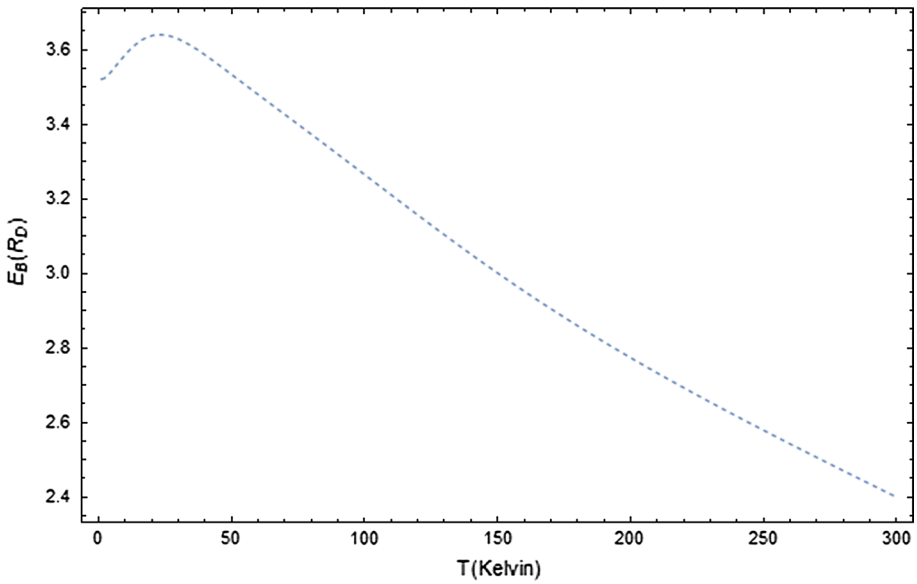

Fig. 4 3D average binding energy of donor impurity in QD as a function of temperature (T) at constant $R = 2a_D, V_0 = 100R_D$

reduce the binding energy. The maximum value of the binding energy approaches to 3.625 R_D at temperature equals 20 K.

Figure 5 shows the behavior of the heat capacity (C_v) for donor impurity QD versus the temperature (T). The monotonic increase in the heat capacity (C_v) with temperature (T) is expected, but as the temperature (T) is increased from absolute zero, the heat capacity (C_v) suddenly increases and then decreases giving a peak-like structure. The peak structure is the well-known Schottky anomaly of the heat capacity (C_v), typical for a system where only two states are importance at low temperature (T) because the thermal energy gained by electrons is enough for only the lowest two levels. The increase in heat capacity (C_v) with temperature (T) can be attributed to the increase in the thermal energy ($E_{th}=k_BT$) for electrons which makes more and more states available for thermal excitation. However, as the temperature (T) keeps increasing, the heat capacity finally saturates where all the energy levels are populated evenly (there no substantial change). The saturation value of the heat capacity (C_v) approaches at room temperature (300 K) is found to be about 0.825 K_β.

In Fig. 6, we show the dependence of the thermal heat capacity (C_v) of donor impurity QD on the temperature (T) for different values of confinement potential depth (V_0) while keeping R unchanged. As increases (V_0)(more confinement energy), the excitation energies for the low-lying excited states become large, so the environments thermal energy will not excite the system and that leads to a very low heat capacity (C_v).

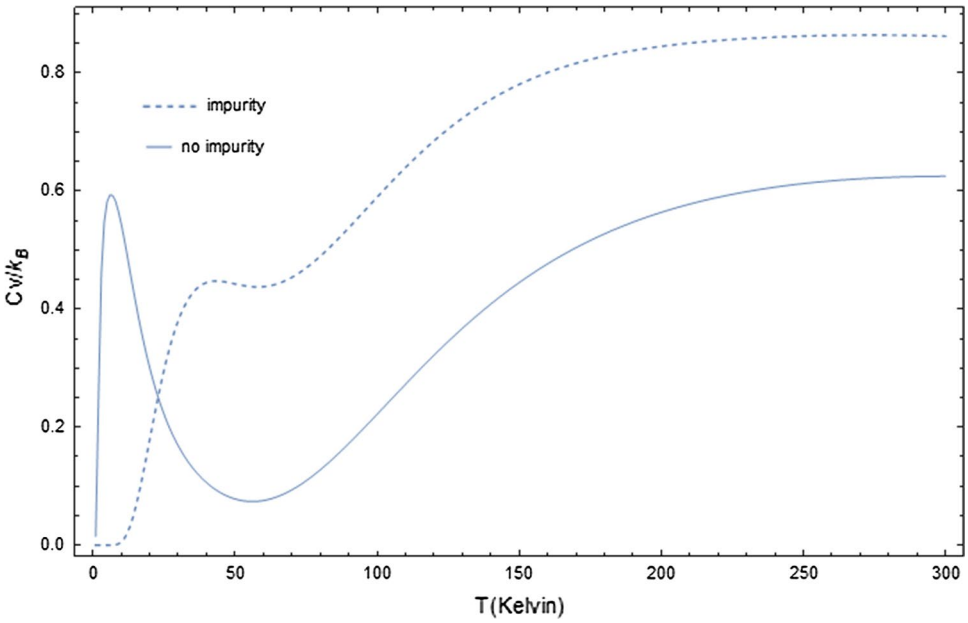

Fig. 5 Heat capacity of QD (C_v/k_B) as a function of temperature (T) with donor impurity and without impurity at constant $R = 2a_D, V_0 = 100R_D, N = 3D$

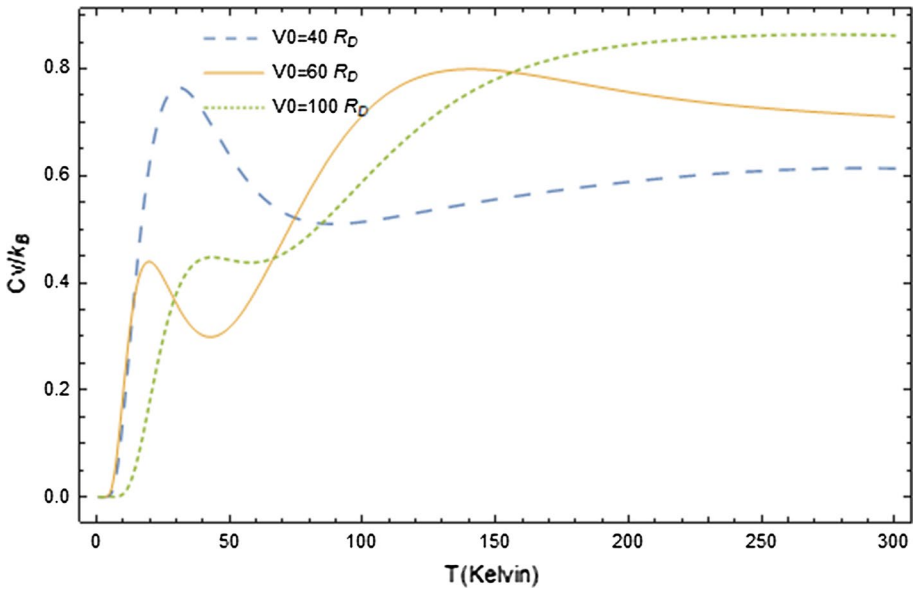

Fig. 6 Heat capacity of donor impurity QD (C_v/k_B) as a function of temperature (T) for different values $V_0 = 40R_D, 60R_D, 100R_D$ at constant $R = 2a_D, N = 3D$

The heat capacity (C_v) of donor impurity QD as a function of temperature (T) for different values of QD radius (R) is presented in Fig. 7. It is important to note that no direct sequence of the location of the Schottky temperature with the QD parameters V_0 and R is noticed. Figure 8 shows the dependence of the heat capacity (C_v) of donor impurity QD on the dimension (N) for fixed values of (V_0) and (R). We can see that heat capacity curves cross at the same temperature point which almost equals 170 K (energy-level crossing). As the dimensionality of the QD reduces, the energy of the QD enhances and in this case the heat capacity decreases since more thermal energy is required to excite the electron.

Another important thermodynamics quantity we have studied is the entropy (S). We have calculated the entropy (S) as a function of temperature (T) as shown in Fig. 9 with impurity and without impurity. The enhancement in the entropy (S) of the QD as the temperature (T) increases is expected. At lower temperatures, the behavior is qualitatively different as compared to that at relatively higher temperatures; the entropy increases monotonically at high value of temperatures, but at low temperatures the entropy increases quite rapidly. The thermal energy of electrons will bring more and more disorder in the form of random motion, so the entropy (S) increases with temperature (T) increasing. At zero

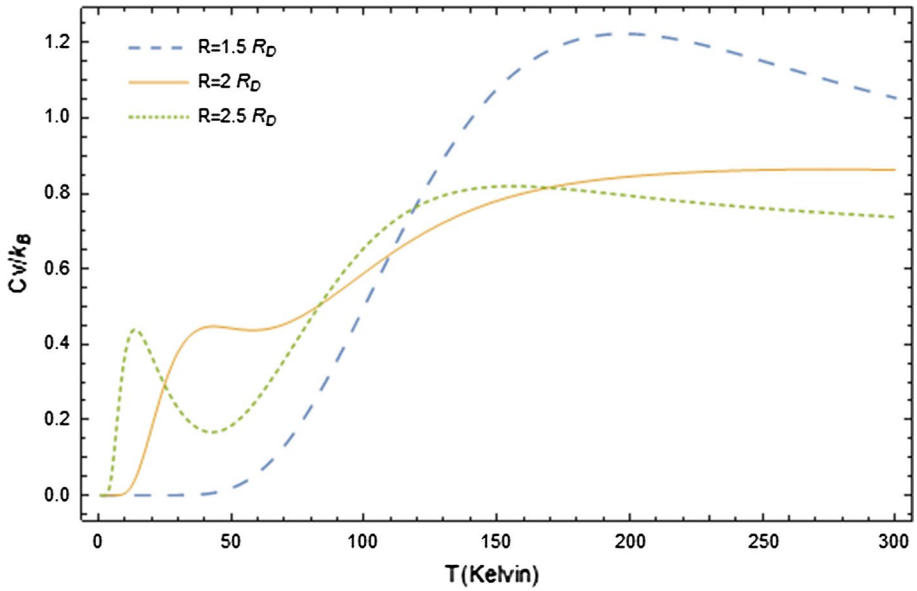

Fig. 7 Heat capacity of donor impurity QD (C_v/k_B) as a function of temperature (T) for different values of $R = 1.5a_D, 2a_D, 2.5a_D$ at constant $V_0 = 100R_D, N = 3D$

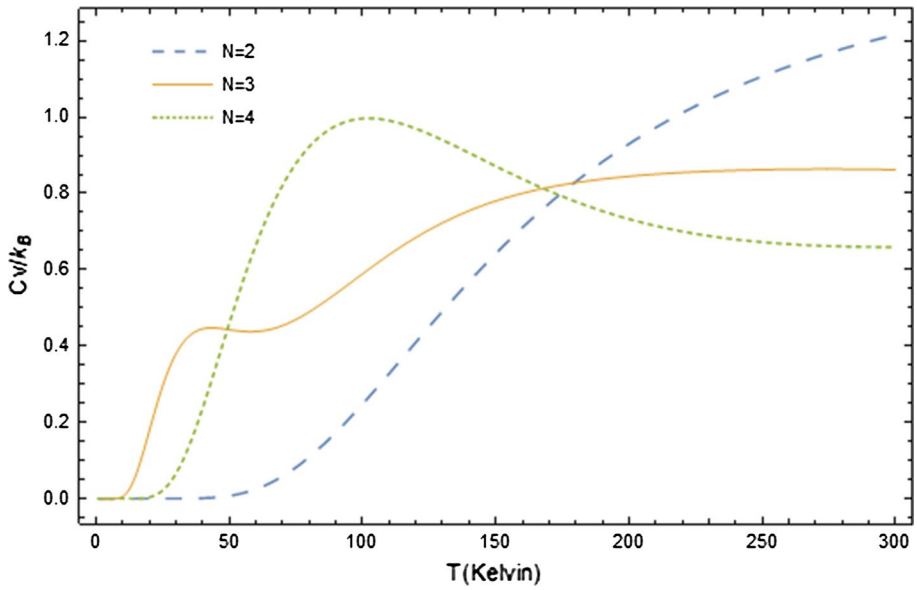

Fig. 8 Heat capacity of donor impurity QD (C_v/k_B) as a function of temperature (T) for different values of $N = 2D, 3D, 4D$ at constant $V_0 = 100R_D, R = 2a_D$

temperature (T), only the lowest energy level is occupied, so the entropy (S) is zero and there is a very little probability of a transition to a higher energy level. As the temperature (T) increases, there is an increase in entropy (S) and thus the probability of a transition goes up. We observe also that the presence of the impurity in the QD greatly reduces the entropy (S) of the QD, since the electron is becoming more bound and in this case the disorder decreases leading to a significant reduction in the entropy (S) of the QD.

The variation of entropy (S) with respect to the QD radius (R) at different temperatures (T) is shown in Fig. 10. The figure shows that the entropy (S) increases as the QD radius (R) increases because the increase in radius will lead to the more ways there are to distribute the atom in that size which means higher entropy (S). Figure 11 shows the effect of the potential depth $\left(V_0\right)$ on the behavior of the curve of the entropy (S) at different temperatures (T). The figure shows clearly the change in the entropy (S) curves as we increase the confining Gaussian potential V_0. The Gaussian potential term $(-V_0 e^{-r^2/2R^2})$ enhancing greatly the total energy state due to its large Gaussian energy confinement.

To emphasize the effect of dimension (N) on entropy (S), we plot in Fig. 12 the entropy S/k_B as a function of temperature (T) but at different values of dimension (N). The entropy change is due to the difference in spectral density of QD states.

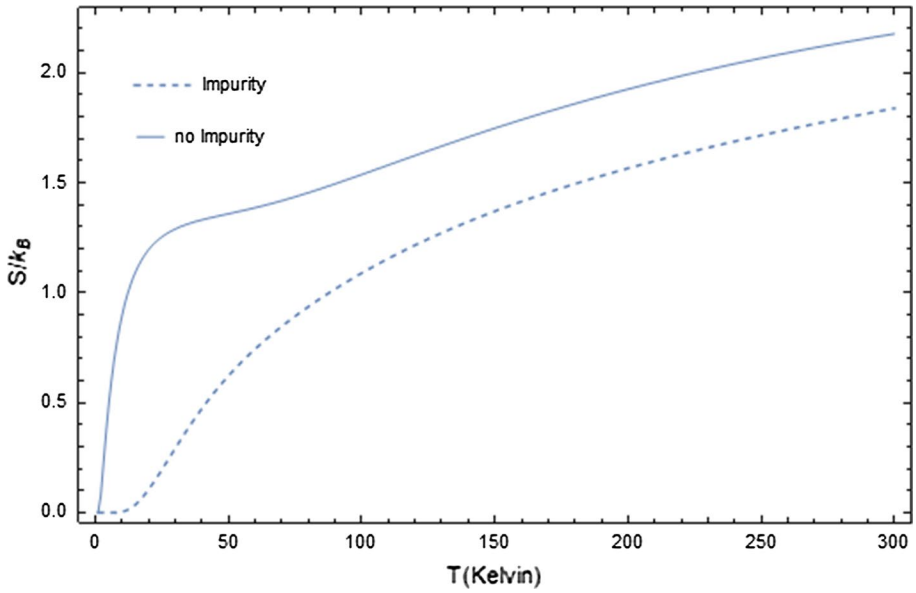

Fig. 9 Entropy of QD (S/k_{B}) as a function of temperature (T) with donor impurity and without impurity at constant $R = 2a_{\mathrm{D}}, V_0 = 50R_{\mathrm{D}}, N = 3D$

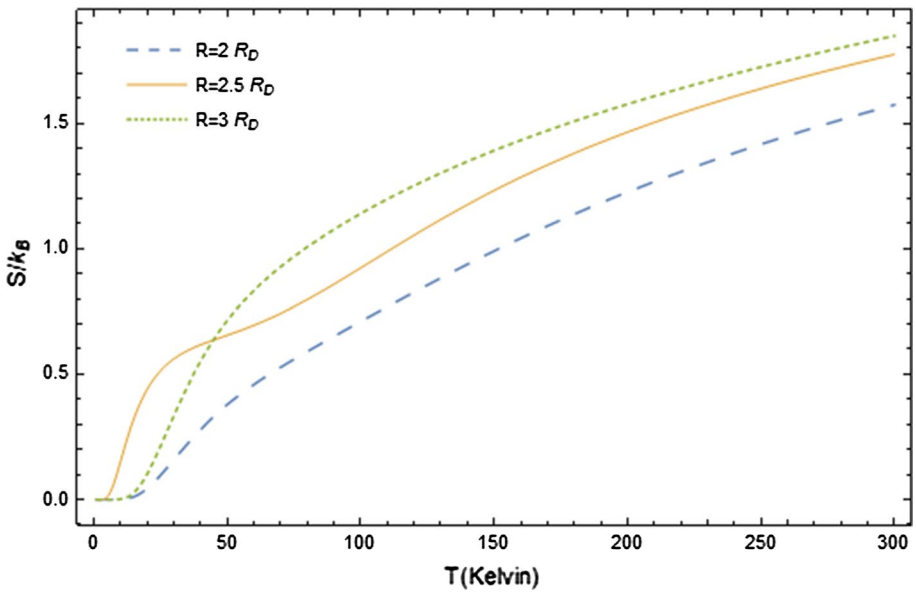

Fig. 10 Entropy of donor impurity in QD (S/k_{B}) as a function of temperature (T) for different values of $R = 1.5a_{\mathrm{D}}, 2a_{\mathrm{D}}, 2.5a_{\mathrm{D}}$ at constant $V_0 = 100R_D, N = 3D$.

Conclusions

We have solved the Hamiltonian of GaAs/AlGaAs spherical QD, in the presence of donor impurity and Gaussian confining potential using the shifted $1/N$ expansion method. We have presented a calculation for the donor energies in quantum dot of different dimensions, $N = 2$, 3 and 4. The effects of impurity on the ground state energy and average energy have been considered. The computed result shows that the donor impurity increases effectively the average energy due to its negative Coulomb contribution. According to the numerical results obtained in this work, we have shown the shifted $1/N$ expansion method is very efficient and accurate in calculating the energy spectrum of the donor impurity in QD. The heat capacity (C_v) and entropy (S) dependence on dot radius (R), confining potential depth (V_0), dimension (N) and temperature (T) of GaAs/AlGaAs QD have been investigated. The investigations had shown clearly that as we increase the temperature (T), dot radius (R) and dimension (N), the heat capacity (C_v) and entropy (S) enhance, while increasing the confining potential depth (V_0) leads to a reduction in QD-thermal quantities: the heat capacity (C_v) and entropy (S).

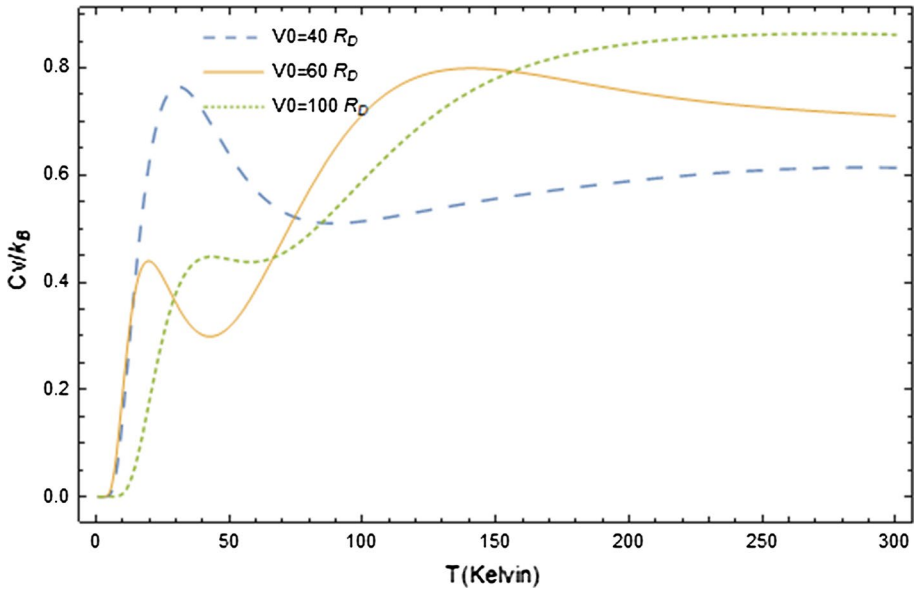

Fig. 11 Entropy of donor impurity in QD (S/k_B) as a function of temperature (T) for different values of $V_0 = 40R_D, 60R_D, 100R_D$ at constant $R = 2.5a_D, N = 3D$

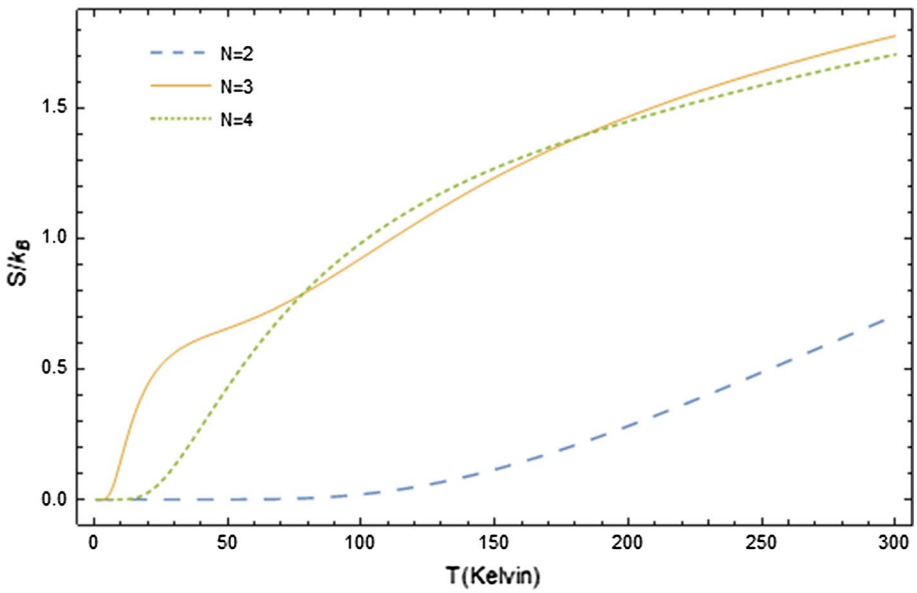

Fig. 12 Entropy of donor impurity in QD (S/k_B) as a function of temperature (T) for different values of $N = 2D, 3D, 4D$ at constant $R = 2.5a_D, V_0 = 100R_D$

Appendix

The shifted $1/N$ expansion method consists in solving Eq. (5) systematically in terms of the expansion parameter $1/\bar{k}$. The leading contribution to the energy comes from the effective potential:

$$V_{\text{eff}}(r) = \frac{\hbar^2}{8m^* r^2} + \frac{V(r)}{Q} \tag{14}$$

where Q is a constant which rescales the potential (in large $\bar{k}$ limit), $Q = \bar{k}^2$. To obtain such an expansion, it is necessary to remove linear parts with respect to the coordinates in the potential. Therefore, we develop the potential around its minimum.

$V(r)$ is assumed to be well behaved so that $V_{\text{eff}}(r)$ has minimum at $r = r_0$ and there are well-defined bound states. Q is then determined from the following equation:

$$4m^* r_0^3 V'(r_0) = \hbar^2 Q \tag{15}$$

In order to shift the origin of the coordinate to the position of the minimum of the effective potential, it is convenient to define a new variable x

$$x = \frac{\bar{k}^{\frac{1}{2}}}{r_0}\left(r - r_0\right) \tag{16}$$

By using the Taylor expansion around the effective potential minimum r_0, respectively $x = 0$, we obtain an analytical equation similar to the Schrodinger equation of the one-dimensional anharmonic solvable oscillator. We compare the coefficients of both equations to define all the anharmonic oscillator parameters in terms of $\bar{k}$, Q, r_0 and the potential derivatives in order to obtain the energy spectrum.

We will define an oscillator frequency:

$$\omega = \frac{\hbar}{2m^*}\left[3 + \frac{r_0 V''\left(r_0\right)}{V'\left(r_0\right)}\right]^{1/2} \tag{17}$$

The energy eigenvalues are given by an expansion in powers of $1/\bar{k}$ where $\bar{k} = N + 2l - a$, N being the number of spatial dimensions and (a) so-called shifted parameter.

The shift parameter is defined by equation:

$$a = 2 - 2\left(2n_r + 1\right)\frac{m^*\omega}{\hbar} \tag{18}$$

For any value of the radial quantum number n_r and for any value of l, the energy $E\left(n_r, l\right)$ (up to third order of $1/\bar{k}$) is given by:

$$E(n,l) = E_0 + E_1 + E_2 + E_3. \tag{19}$$

The binding energy $E_{\mathrm{B}}(n,l)$ in a given state is defined by

$$E_{\mathrm{B}}(n,l) = E_{\mathrm{B}}(n,l,z=0) - E_{\mathrm{B}}(n,l,z=1)$$

where

$$E_0 = V(r) + \left(Q/\left(8 * m^* * r^2\right)\right.$$
$$E_1 = \left(c_1 * c_3\right)/(8 * m^*)$$
$$E_2 = \left(E_1 + \alpha_1\right)/r^2$$
$$E_3 = \alpha_2/\left(\bar{k} * r^2\right)$$

where

$$Q = (N + 2 * \ell - a)^2$$
$$c_1 = (1 - a)$$
$$c_2 = (2 - a)$$
$$c_3 = (3 - a)$$
$$\alpha_1 = n_1 * e_2 + 3 * n_2 * e_4 - c_5 * \left(e_1^2 + 6 * n_1 * e_1 * e_3 + n_4 * e_3^2\right)$$
$$\alpha_2 = t_7 + t_{12} + t_{16}$$
$$c_5 = \omega^{-1}$$

The explicit forms of the previous parameters are given in the following

$$t_7 = t_1 - c_5 * \left(t_2 + t_3 + t_4 + t_5 + t_6\right)$$
$$t_{12} = c_5^2 * \left(t_8 + t_9 + t_{10} + t_{11}\right)$$
$$t_{16} = -c_5^3 * \left(t_{13} + t_{14} + t_{15}\right)$$

with

$$t_1 = n_1 * d_2 + 3 * n_2 * d_4 + 5 * n_3 * d_6$$
$$t_2 = n_1 * e_2^2 + 12 * n_2 * e_2 * e_4$$
$$t_3 = 2 * e_1 * d_1 + 2 * n_5 * e_4^2$$
$$t_4 = 6 * n_1 * e_1 * d_3 + 30 * n_2 * e_1 * d_5$$
$$t_5 = 6 * n_1 * e_3 * d_1 + 2 * n_4 * e_3 * d_3$$
$$t_6 = 10 * n_6 * e_3 * d_5$$
$$t_8 = 4 * e_1^2 * e_2 + 36 * n_1 * e_1 * e_2 * e_3$$
$$t_9 = 8 * n_4 * e_2 * e_3^2$$
$$t_{10} = 24 * n_1 * e_1^2 * e_4 + 8 * n_7 * e_1 * e_3 * e_4$$
$$t_{11} = 12 * n_8 * e_3^2 * e_4$$
$$t_{13} = 8 * e_1^3 * e_3 + 108 * n_1 * e_1^2 * e_3^2$$
$$t_{14} = 48 * n_4 * e_1 * e_3^3$$
$$t_{15} = 30 * n_9 * e_3^4$$

where $(n{\cdot}s)(d{\cdot}s)$ and $(e{\cdot}s)$ are parameters given as:

$$n_1 = 1 + 2 * n_r$$
$$n_2 = 1 + 2 * n_r + 2 * n_r^2$$
$$n_3 = 3 + 8 * n_r + 6 * n_r^2 + 4 * n_r^3$$
$$n_4 = 11 + 30 * n_r + 30 * n_r^2$$
$$n_5 = 21 + 59 * n_r + 51 * n_r^2 + 34 * n_r^3$$
$$n_6 = 13 + 40 * n_r + 42 * n_r^2 + 28 * n_r^3$$
$$n_7 = 31 + 78 * n_r + 78 * n_r^2$$
$$n_8 = 57 + 189 * n_r + 225 * n_r^2 + 150 * n_r^3$$
$$n_9 = 31 + 109 * n_r + 141 * n_r^2 + 94 * n_r^3$$
$$c_4 = 2 * m^* * \omega$$
$$e_1 = \epsilon_1/\sqrt{c_4}$$
$$e_2 = \epsilon_2/c_4$$
$$e_3 = \epsilon_3/c_4^{3/2}$$
$$e_4 = \epsilon_4/c_4^2$$
$$d_1 = \delta_1/\sqrt{c_4}$$
$$d_2 = \delta_2/c_4$$
$$d_3 = \delta_3/c_4^{3/2}$$
$$d_4 = \delta_4/c_4^2$$
$$d_5 = \delta_5/c_4^{5/2}$$
$$d_6 = \delta_6/c_4^3$$

Furthermore:

$$\epsilon_1 = c_2/(2 * m^*)$$
$$\epsilon_2 = -3 * c_2/(4 * m^*)$$
$$\epsilon_3 = -1/(2 * m^*) + \big(r_5 * \mathrm{der}_3(r)\big)/(6 * Q)$$
$$\epsilon_4 = 5/(8 * m^*) + \big(r_6 * \mathrm{der}_4(r)\big)/(24 * Q)$$
$$\delta_1 = -c_1 * c_3/(4 * m^*)$$
$$\delta_2 = 3 * c_1 * c_3/(8 * m^*)$$
$$\delta_3 = c_2/m^*$$
$$\delta_4 = -5 * c_2/(4 * m^*)$$
$$\delta_5 = -3/(4 * m^*) + \big(r_7 * \mathrm{der}_5(r)\big)/(120 * Q)$$
$$\delta_6 = 7/(8 * m^*) + \big(r_8 * \mathrm{der}_6(r)\big)/(720 * Q)$$

where

$$\mathrm{der}_1(r) = \frac{\mathrm{d}V}{\mathrm{d}r}$$
$$\mathrm{der}_2(r) = \frac{\mathrm{d}^2V}{\mathrm{d}r}$$
$$\mathrm{der}_3(r) = \frac{\mathrm{d}^3V}{\mathrm{d}r^3}$$
$$\mathrm{der}_4(r) = \frac{\mathrm{d}^4V}{\mathrm{d}r^4}$$
$$\mathrm{der}_5(r) = \frac{\mathrm{d}^5V}{\mathrm{d}r^5}$$
$$\mathrm{der}_6(r) = \frac{\mathrm{d}^6V}{\mathrm{d}r^6}$$

References

1. Maksym, P.A., Chakraborty, T.: Quantum dots in a magnetic field: role of electron–electron interactions. Phys. Rev. Lett. **65**(1), 108 (1990)
2. De Groote, J.J.S., Hornos, J.E.M., Chaplik, A.V.: Thermodynamic properties of quantum dots in a magnetic field. Phys. Rev. B **46**(19), 12773 (1992)
3. Pfannkuche, D., Gudmundsson, V., Maksym, P.: A comparison of a Hartree, a Hartree–Fock, and an exact treatment of quantum-dot helium. Phys. Rev. B **47**(4), 2244 (1993)
4. Castaño-Yepes, J.D., Ramirez-Gutierrez, C.F., Correa-Gallego, H., Gómez, E.A.: A comparative study on heat capacity, magnetization and magnetic susceptibility for a GaAs quantum dot with asymmetric confinement. Physica E **103**, 464–470 (2018)
5. Atoyan, M.S., Kazaryan, E.M., Sarkisyan, H.A.: Interband light absorption in parabolic quantum dot in the presence of electrical and magnetic fields. Physica E **31**(1), 83–85 (2006)
6. Ikhdair, S.M., Hamzavi, M., Sever, R.: Spectra of cylindrical quantum dots: the effect of electrical and magnetic fields together with AB flux field. Physica B **407**(23), 4523–4529 (2012)
7. Shaer, A., Elsaid, M.K., Elhasan, M.: Magnetization of GaAs parabolic quantum dot by variation method. J. Phys. Sci. Appl. **6**(2), 39–46 (2016)
8. Nguyen, N.T., Sarma, S.D.: Impurity effects on semiconductor quantum bits in coupled quantum dots. Phys. Rev. B **83**(23), 235322 (2011)
9. Chuu, D.S., Hsiao, C.M., Mei, W.N.: Hydrogenic impurity states in quantum dots and quantum wires. Phys. Rev. B **46**(7), 3898 (1992)
10. Zhu, J.L.: Exact solutions for hydrogenic donor states in a spherically rectangular quantum well. Phys. Rev. B **39**(12), 8780 (1989)
11. MacDonald, A.H., Ritchie, D.S.: Hydrogenic energy levels in two dimensions at arbitrary magnetic fields. Phys. Rev. B **33**(12), 8336 (1986)
12. Sarkar, S., Sarkar, S., Bose, C.: Influence of polarization and self-polarization charges on impurity binding energy in spherical quantum dot with parabolic confinement. Physica B **541**, 75–78 (2018)
13. Liang, S.J., Xie, W.F.: The hydrostatic pressure and temperature effects on a hydrogenic impurity in a spherical quantum dot. Eur. Phys. J. B **81**(1), 79–84 (2011)
14. Bose, C.: Binding energy of impurity states in spherical quantum dots with parabolic confinement. J. Appl. Phys. **83**(6), 3089–3091 (1998)
15. Bose, C., Sarkar, C.K.: Perturbation calculation of donor states in a spherical quantum dot. Solid State Electron. **42**(9), 1661–1663 (1998)
16. Xie, W.: Negative donor centers in a GaAs parabolic quantum dot. Phys. Lett. A **263**(1–2), 127–130 (1999)
17. Zhu, J.L., Xiong, J.J., Gu, B.L.: Confined electron and hydrogenic donor states in a spherical quantum dot of GaAs-$Ga_{1-x}Al_xAs$. Phys. Rev. B **41**(9), 6001 (1990)
18. Zhu, J.L., Wu, J., Fu, R.T., Chen, H., Kawazoe, Y.: Effects of quantum size and potential shape on the spectra of an electron and a donor in quantum dots. Phys. Rev. B **55**(3), 1673 (1997)
19. Bose, C., Sarkar, C.K.: Effect of a parabolic potential on the impurity binding energy in spherical quantum dots. Physica B **253**, 238–241 (1998)
20. Porras-Montenegro, N., Pe, S.T.: Hydrogenic impurities in GaAs-(Ga, Al) as quantum dots. Phys. Rev. B **46**(15), 9780 (1992)
21. Movilla, J.L., Planelles, J.: Image charges in spherical quantum dots with an off-centered impurity: algorithm and numerical results. Comput. Phys. Commun. **170**(2), 144–152 (2005)
22. Reimann, S.M., Manninen, M.: Electronic structure of quantum dots. Rev. Mod. Phys. **74**(4), 1283 (2002)
23. Avetisyan, S., Chakraborty, T., Pietiläinen, P.: Magnetization of interacting electrons in anisotropic quantum dots with Rashba spin–orbit interaction. Physica E **81**, 334–338 (2016)
24. Boyacioglu, B., Chatterjee, A.: Dia- and paramagnetism and total susceptibility of GaAs quantum dots with Gaussian confinement. Physica E **44**(9), 1826–1831 (2012)
25. Boyacioglu, B., Chatterjee, A.: Magnetic properties of semiconductor quantum dots with gaussian confinement. Int. J. Mod. Phys. B **26**(04), 1250018 (2012)
26. Castaño-Yepes, J.D., Amor-Quiroz, D.A., Ramirez-Gutierrez, C.F., Gómez, E.A.: Impact of a topological defect and Rashba spin–orbit interaction on the thermo-magnetic and optical properties of a 2D semiconductor quantum dot with Gaussian confinement. Physica E **109**, 59–66 (2019)
27. Madhav, A.V., Chakraborty, T.: Electronic properties of anisotropic quantum dots in a magnetic field. Phys. Rev. B **49**(12), 8163 (1994)
28. Gharaati, A., Khordad, R.: A new confinement potential in spherical quantum dots: modified Gaussian potential. Superlattices Microstruct. **48**(3), 276–287 (2010)
29. Boda, A., Chatterjee, A.: Ground state and binding energies of (D^0), (D^-) centres and resultant dipole moment of a (D^-) centre in a GaAs quantum dot with Gaussian confinement. Physica E **45**, 36 (2012)

30. Sukhatme, U., Imbo, T.: Shifted 1/*N* expansions for energy eigenvalues of the Schrödinger equation. Phys. Rev. D **28**(2), 418 (1983)
31. Imbo, T., Pagnamenta, A., Sukhatme, U.: Energy eigenstates of spherically symmetric potentials using the shifted 1/*N* expansion. Phys. Rev. D **29**(8), 1669 (1984)
32. El-Said, M.: Energy states of two electrons in a parabolic quantum dot in a magnetic field. J. Phys. I **5**, 1027–1036 (1995)
33. El-Said, M.: The ground-state electronic properties of a quantum dot with a magnetic field. Phys. Scr. **75**, 436 (2007)
34. Wang, S., Kang, Y., Li, X.L.: Binding energy of the ground and first few excited states of hydrogenic donor impurity in a rectangular GaAs quantum dot in the presence of electric field. Superlattices Microstruct. **76**, 221–233 (2014)
35. Gomez, S., Romero, R.: Few-electron semiconductor quantum dots with Gaussian confinement. Open Phys. **7**(1), 12–21 (2009)
36. Thijssen, J.M.: Computational Physics. Cambridge University Press, Cambridge (1999)
37. Lai, C.S.: On the Schrodinger equation for the gaussian potential-A exp $(-\lambda r^2)$. J. Phys. A Math. Gen. **16**(6), L181 (1983)
38. Nammas, F.S.: Thermodynamic properties of two electrons quantum dot with harmonic interaction. Physica A **508**, 187–198 (2018)